Original Article

DOI: 10.5582/bst.2023.01164

The function and immune role of cuproptosis associated hub gene in Barrett's esophagus and esophageal adenocarcinoma

Kailin Lin[1,2,3,§], Ke Hu[4,§], Qiwen Chen[3], Jiangchun Wu[3,5,*]

[1] Departments of Thoracic Surgery and State Key Laboratory of Genetic Engineering, Fudan University Shanghai Cancer Center, Shanghai, China;
[2] Institute of Thoracic Oncology, Fudan University, Shanghai, China;
[3] Department of Oncology, Shanghai Medical College, Fudan University, Shanghai, China;
[4] Department of Endocrinology, Minhang Hospital, Fudan University Shanghai, China;
[5] Department of Gynecologic Oncology, Fudan University Shanghai Cancer Center, Fudan University, Shanghai, China.

SUMMARY Barrett's esophagus (BE) is a precancerous lesion of esophageal adenocarcinoma (EAC), with approximately 3-5% of patients developing EAC. Cuproptosis is a kind of programmed cell death phenomenon discovered in recent years, which is related to the occurrence and development of many diseases. However, its role in BE and EAC is not fully understood. We used single sample Gene Set Enrichment Analysis (ssGSEA) for differential analysis of BE in the database, followed by enrichment analysis of Kyoto Encyclopedia of Genes and Genomes (KEGG), Gene Ontology (GO) and GSEA, Protein-Protein Interaction (PPI), Weighted Gene Co-expression Network Analysis (WGCNA), Receiver Operating Characteristic Curve (ROC) and finally Quantitative Real Time Polymerase Chain Reaction (qRT-PCR) and immunohistochemistry (IHC) of clinical tissues. Two hub genes can be obtained by intersection of the results obtained from the cuproptosis signal analysis based on BE. The ROC curves of these two genes predicted EAC, and the Area Under the Curve (AUC) values could reach 0.950 and 0.946, respectively. The mRNA and protein levels of Centrosome associated protein E (CENPE) and Shc SH2 domain binding protein 1 (SHCBP1) were significantly increased in clinical EAC tissues. When they were grouped by protein expression levels, high expression of CENPE or SHCBP1 had a poor prognosis. The CENPE and SHCBP1 associated with cuproptosis may be a factor promoting the development of BE into EAC which associated with the regulation of NK cells and T cells.

Keywords Barrett's esophagus, cuproptosis, hub gene, esophageal adenocarcinoma, immunoinfiltration

1. Introduction

Barrett's esophagus (BE) is characterized by the replacement of normal esophageal squamous cell epithelium with columnar metaplasia and affects approximately 1% worldwide (*1,2*). The incidence of BE associated esophageal adenocarcinoma (EAC) is on the increase. Approximately 3% to 5% of patients with BE will be diagnosed with EAC during their lifetime (*3,4*). However, the specific mechanism of BE that leads to EAC is not yet fully understood.

Cuproptosis is a novel copper ion-dependent cell death type being regulated in cells, and this is quite different from the common cell death patterns such as apoptosis, necroptosis, ferroptosis and pyroptosis (*5,6*). Recently, cuproptosis-related genes have recently been reported to regulate the occurrence and progression of various tumors (*7-10*). The role of cuproptosis in BE in the development of EAC has not been reported yet.

Centrosome associated protein E (CENPE) is a positive end-directed kinetoprotein belonging to the kinase-7 subfamily and plays a key role in mitosis (*11-13*). Studies have reported that the expression of CENPE in EAC is significantly higher than that of pan-cancer, which is related to DNA methylation in EAC and is a negative prognostic factor for patients (*11*). Shc SH2 domain binding protein 1 (SHCBP1) is a SH2 domain specific binding protein (Shc) of Src homologues and collagen homologues, which is mainly involved in the regulation of various signal transduction pathways and plays an important role in cell signal transduction (*14*). SHCBP1 can be used as an immune marker for pan-cancer diagnosis, which is negatively correlated with patient prognosis and can be used as a target for immunotherapy (*14,15*). Recent studies suggest that the high expression of SHCBP1 may be

related to the immunosuppressive microenvironment of tumors, providing a potential new target for tumor immunotherapy (*16,17*). However, the role of CENPE or SHCBP1 in BE, EAC, and BE transformation into EAC has not been reported yet.

In this study, by mining BE cuprotosis related gene modules, CENPE and SHCBP1, markers of BE progression into EAC, were screened out, and verified by gene expression difference, survival analysis and ROC curve. Then, we further verified the clinical samples of our center and analyzed the prognosis, and the results were consistent with previous research reports. By single cell analysis, it was found that CENPE and SHCBP1 were co-expressed on NK cells and T cells, which may relate to the immune function of NK cells and T cells. Therefore, this study deeply analyzed the mechanism of BE developing into EAC through cuprotosis.

2. Materials and Methods

2.1. Data collection

The mRNA expression data of BE (GSE26886) and EAC were downloaded from Gene Expression Omnibus (GEO) database (*https://www.ncbi.nlm.nih.gov/geo/*) and The Cancer Genome Atlas (TCGA) (*https://portal.gdc.cancer.gov/*) database (*18*). All cuproptosis-related marker genes were obtained from the study of Tsvetkov *et al*. (*19*).

2.2. Single sample Gene Set Enrichment Analysis (ssGSEA)

The ssGSEA analysis was commonly performed using Gene Set Variation Analysis (GSVA) package (*20*). Cuproptosis-related genes were considered as a reference gene set, and normalized gene expression data were inputted. Finally, the cuproptosis-related score of each sample was calculated.

2.3. Differential analysis and Weighted Gene Co-expression Network Analysis (WGCNA)

We conducted differential analysis by the limma package for cuproptosis-related score. The screening conditions for the differentially expressed genes (DEG) were: $|\log^2$ (fold change) $| > 1$ and adjusted $P < 0.05$. Then, we drew the volcano maps and heatmaps with the R package "ggplot2" and "pheatmap" to visualize DEGs (*21*). Moreover, we used the WGCNA package to create a gene co-expression network based on the cuproptosis-related score (*22*). Firstly, we built the adjacency matrix using soft-threshold 7 and the topological overlap matrix (TOM). Then the model eigengene was calculated, as well as the correlation between models and clinical traits. Finally, the positively related gene models were selected.

2.4. Functional enrichment analysis

Gene Ontology (GO) (*23*), the Kyoto Encyclopedia of Genes and Genomes (KEGG) (*24*) and Gene Set Enrichment Analysis (GSEA) (*25*) were performed using "clusterProfiler" package. $*P < 0.05$ as a threshold for significantly enriched GO terms and KEGG pathways and adjusted $*P < 0.05$ for GSEA. cBio Cancer Genomics Portal (cBioPortal) (*http://cbioportal.org*) have collected a multidimensional cancer genomics data set. The type and frequency of target genes mutation in tumors were analyzed in "OncoPrint" and "Cancer Types Summary." "OncoPrint" shows the mutation, copy number, and expression of the target gene in the samples in the heatmap. In addition, "Cancer Types Summary" shows the mutation rate of the target genes in a bar chart.

2.5. Patient cohort

All patients for whom samples were collected obtained informed consent from the patient prior to collection. All operations and procedures are in accordance with the rules of the Institutional Ethics Review Committee of the World Health Organization (WHO) Collaborating Centre for Human Production Research and the authorization of the Human Ethics Committee of Fudan University Shanghai Cancer Center (FUSCC).

All EAC sample and benign esophageal were obtained from patients who underwent Esophagostomy without chemotherapy or radiotherapy before surgery between 2012 and 2018, all tissues were surgically removed, and pathological results were reviewed, scored and recorded by experienced pathologists in our center. All clinical records were retrospectively studied.

2.6. qRT-PCR

The total RNA extraction of tissues was performed using RNA extraction kits (QIAGEN, Germany) according to the manufacturer's protocol. qRT-PCR was performed using the Bio-Rad CFX96 Real-Time PCR operating instrument with SYBR qPCR Mix (Takara, Dalian, China). The original Ct values of the target genes CENPE and SHCBP1 were obtained according to the PCR standard reaction curve, and the $2^{-\Delta\Delta Ct}$ method was applied for semi-quantitative analysis. The relative expression of CENPE and SHCBP1 was normalized with GAPDH. The primer sequences are as follows: CENPE-F: 5' -GCTACCGTGATAAACCAGGTTC-3', CENPE-R: 5' -AGGCTCTGAATCGCTCATAGA-3', SHCBP1-F: 5' -GATTCTGCCATACAAGGCTACAA-3', SHCBP1-R: 5' -TGCCCTGGGTATAACTCCCAA-3', SLC31A1-F: GGGGATGAGCTATATGGACTCC, SLC31A1-R: TCACCAAACCGGAAAACAGTAG, GAPDH-F: 5' -GGAGCGAGATCCCTCCAAAAT-3', GAPDH-R: 5' -GGCTGTTGTCATACTTCTCATGG-3'.

2.7. Immunohistochemical (IHC) and immunoreactivity score (IRS)

IHC was used to detect the expression of hub genes (CENPE and SHCBP1) in esophageal cancer tissues. The slice thickness was set at 5 μm, and 3 sections were selected from each specimen. Slides were rinsed and incubated with primary antibodies against CENPE and SHCBP1 (CENPE: 1:1000, abcam, ab5093; SHCBP1: 1:1000, abcam, ab184467). Subsequent antibody detection was carried out with a Cy3-conjugated goat anti-rabbit/mouse secondary antibody (1:300; Invitrogen) (26-28).

The tissue chip (TMA) included 148 normal tissue samples and 164 esophageal cancer tissue samples. TMA was scanned and analyzed by immunoreactivity score (IRS) scoring method. The expression of Hub protein was divided into four levels: 0 (negative), 1 (weakly positive), 2 (moderately positive), and 3 (strongly positive) (*29,30*).

2.8. Survival analysis

Patients with negative (N) and weak positive (W) expression of Hub were included in the low Hub expression group, and patients with moderate positive (M) and strong positive (S) expression were included in the high Hub expression group. The primary outcome of overall survival (OS) was defined as the time from initial treatment to death or the last follow-up, and the secondary end point of progression-free survival (PFS) was defined as the time from initial treatment to disease progression or death (*31-33*). OS and PFS were compared between high-low expression groups.

2.9. Cell lines, culture conditions and treatments

Eca109 and KYSE450 cells were obtained from the American Type Culture Collection (ATCC, Manassas, Virginia, USA) and authenticated by short tandem repeat profiling. All cell lines were cultured at 5% CO_2 and 37°C in high-glucose Dulbecco's modified Eagle's medium (DMEM; Gibco, USA) supplemented with 10% foetal bovine serum (FBS; Gibco, USA) and 1% penicillin-streptomycin (Gibco, USA).

Copper ionophores: Elesclomol (S1052, Selleck, Shanghai, China) was purchased from Selleck (Shanghai, China). Metal ion chloride: Copper (II) chloride ($CuCl_2$, 751944, Sigma-Aldrich, Darmstadt, Germany), were purchased from Sigma-Aldrich Technology (Darmstadt, Germany).

2.10. Stable and transient transfections

For lentivirus production, the packaging vectors psPAX2 and pMD2.G were cotransfected with lentiviral vectors into HEK293T cells using Lipofectamine 3000 (Invitrogen, CA, USA). The virus particles were harvested after transfection for 48 h. Lentiviruses were then transduced into cells with polybrene (2 μg/mL) to increase the infection efficiency. Finally, the positive cells were selected with 2 μg/mL puromycin for 1 week to establish stable cell lines. Synthetic siRNA oligonucleotides were synthesized by Shanghai Genomeditech Co., Ltd. (Shanghai, China). Lipofectamine RNAiMAX (Invitrogen, CA, USA) was used for siRNA transfection. Transient transfection was performed using Lipofectamine 3000 (Invitrogen, CA, USA) according to the manufacturer's instructions. The transfection efficiencies were verified by qRT-PCR and WB.

2.11. Cell viability assays

For the cell proliferation assay, cells were seeded and cultured in 96-well flat-bottom plates, with each well containing 5000 cells in 100 μL. 10 μL Cell Counting Kit-8 (CCK-8) reagent (MedChemExpress, Monmouth Junction, NJ, USA) was added to 90 μl complete culture substrate, and the cell proliferation ability was measured at 450 nm absorption wavelength after 1 hour.

2.12. Intracellular Content of Copper

Intracellular content of copper was measured by copper assay kit (ab272528, Abcam, Boston, MA, USA). Then, 1×10^7 Eca109 cells after elesclomol-$CuCl_2$, shCENPE, shSHCBP1, shSHCBP1-$CuCl_2$, or shSHCBP1-$CuCl_2$ treatment were collected, and they were homogenized after adding 1 ml distilled water. Next, 100 μL samples per well were transferred to a flat-bottom 96-well UV plate. For each assay well, 35 μl Reagent, 5 μL Reagent B and 150 μL Reagent C were thoroughly mixed with samples, incubated for 5 min at room temperature and the optical density read at 359 nm using a microplate reader (Synergy 2, Bio-Tek Instruments, Winooski, VT, USA). Copper content was normalized by protein concentration.

2.13. Western blotting (WB)

Cells were lysed in 10% NP40 (ratio: 890 μL NP40 buffer + 100 μL NP40 + 10 μL protease inhibitor cocktail) (Shanghai Shenger Biotechnology) and lysed in a 4°C centrifuge for 30 minutes (min). Then, the lysates were centrifuged (12,000 g, 4°C, 15 min) to collect the supernatants. The Bio-Rad Protein Assay kit (Hercules, CA, USA) was used to quantify the protein concentration. Approximately 25-30 μg of protein from each sample was separated by 10% SDS–PAGE and electroblotted onto a polyvinylidene fluoride (PVDF) membrane. After blocking with 5% nonfat milk, the membranes were incubated individually overnight at 4°C with the corresponding primary antibodies (SLC31A1

(Abmart Technology, Shanghai, A13469) and β-actin (Sigma-aldrich, #A3854).) and incubated with the secondary antibody, either horseradish peroxidase-conjugated anti-mouse IgG or anti-rabbit, for 1 h at room temperature (RT).

2.14. Immune cell infiltration analysis

Immune cell infiltration analysis was evaluated between high and low cuproptosis-related score using Immuno-Oncology Biological Research (IOBR) package (*34*). In this part, a total of seven algorithms (CIBERSORT, EPIC, MCP, XCELL, ESTIMATE, TIMER, QUANTISEQ) were used. Then, the differences of all immune cell infiltration were visualized by boxplots. Subsequently, we drew a heatmap to show the level of immune cell infiltration.

2.15. Single cell-seq analysis

Single cell-seq data of EAC (GSE173950; Platform: Drop-seq) was downloaded and loaded in R (*35*). Seurat package was used to process the single cell data (*36*). Quality control was performed by calculating the percentage of mitochondria. The threshold of mitochondria was 10%. Then top 2000 variable genes were filtered and normalized. Principal component analysis (PCA) was performed on the scaled data and t-distributed stochastic neighbor embedding (t-SNE) algorithm was performed for cluster identification. The SingleR package was used to annotate all cell types and FindMarkers was used to performed differential analysis (*37-39*).

2.16. Statistical analysis

Statistical analysis was performed with IBM SPSS 23.0 (Chicago, IL, USA), GraphPad Prism 8, and R language. Comparisons between two conditions were based on a two-sided Student's test. OS and PFS curves were plotted with the Kaplan-Meier (KM) method and log-rank test. All the data are shown as the mean ± SD. The results of all statistical analyses were reported as *P* values from two-tailed tests, and $P < 0.05$ was considered to indicate statistical significance (*$P<0.05$, ** $P<0.01$, and *** $P<0.001$).

3. Results

3.1. The results of differential analysis

After data normalization (Figure S1A, *http://www.biosciencetrends.com/action/getSupplementalData.php?ID=171*), we performed differential analysis between high cuproptosis-related score group and low cuproptosis-related score group and finally identified 236 differently expressed genes (57 down regulated and 179 up regulated). Volcano plot showed all the DEGs and top 10 were marked, while the heatmap showed the top 30 DEGs (Figures 1A-B). Then, functional enrichment analyses were performed. We found cell cycle-related biological processes were significantly enriched, such as cell cycle and G2M checkpoint (Figures 1C, 1E, and Figures S1B-D, *http://www.biosciencetrends.com/action/getSupplementalData.php?ID=171*). Moreover, some tumor-associated biological processes were also enriched, for instance E2F targets and MYC targets (Figure 1E). These indicated that cuproptosis-related score was associated with the tumor malignancy. Finally, Protein-Protein Interaction (PPI) network analysis was performed and ten hub genes were identified by cytoHubba (Figure 1D).

3.2. Cuproptosis-related Gene Models of Barrett's Esophagus

A dendrogram of all BE samples with cuproptosis-related score was clustered using average linkage (Figure S2A, *http://www.biosciencetrends.com/action/getSupplementalData.php?ID=171*). Then co-expression analysis was performed to identify gene models and 7 was selected as the soft-threshold (Figure 2A). Based on Spearman correlation coefficient, the heatmap of gene module-trait relationship was drawn to show the correlation between them (Figure 2B). In this study, three gene models (MEsalmon, MEgreen, MEcyan) were positively corrected with the cuproptosis-related score (Figure 2C). Then we combined all the genes and performed functional enrichment analyses and PPI network analysis (Figures 2D-E; Figures S2B-D, *http://www.biosciencetrends.com/action/getSupplementalData.php?ID=171*). We found that cell cycle and metabolism-related pathways were significantly enriched. We surmised that copper ions would intervene tricarboxylic acid cycle and further influence other metabolic processes.

Finally, we took an intersection of the results from DEGs and WGCNA to obtain two hub genes (Fig. 2F).

3.3. Hub genes in EAC

After getting two hub genes, differential analysis, ROC curve and GSEA were performed. Both the CENPE and SHCBP1 were expressed higher in tumor and could be effective biomarkers (Area under curve (AUC) for CENPE: 0.95; AUC for SHCBP1: 0.946; Figures 3A-D). Moreover, the results of single gene GSEA showed that cell proliferation related pathways were significantly enriched, such as cell cycle, DNA replication and p53 signaling pathway (Figures 3E-F).

By analyzing the correlation between CENPE and SHCBP1 in EAC, we found a strong correlation between CENPE and SHCBP1 (Figure 4A). Moreover,

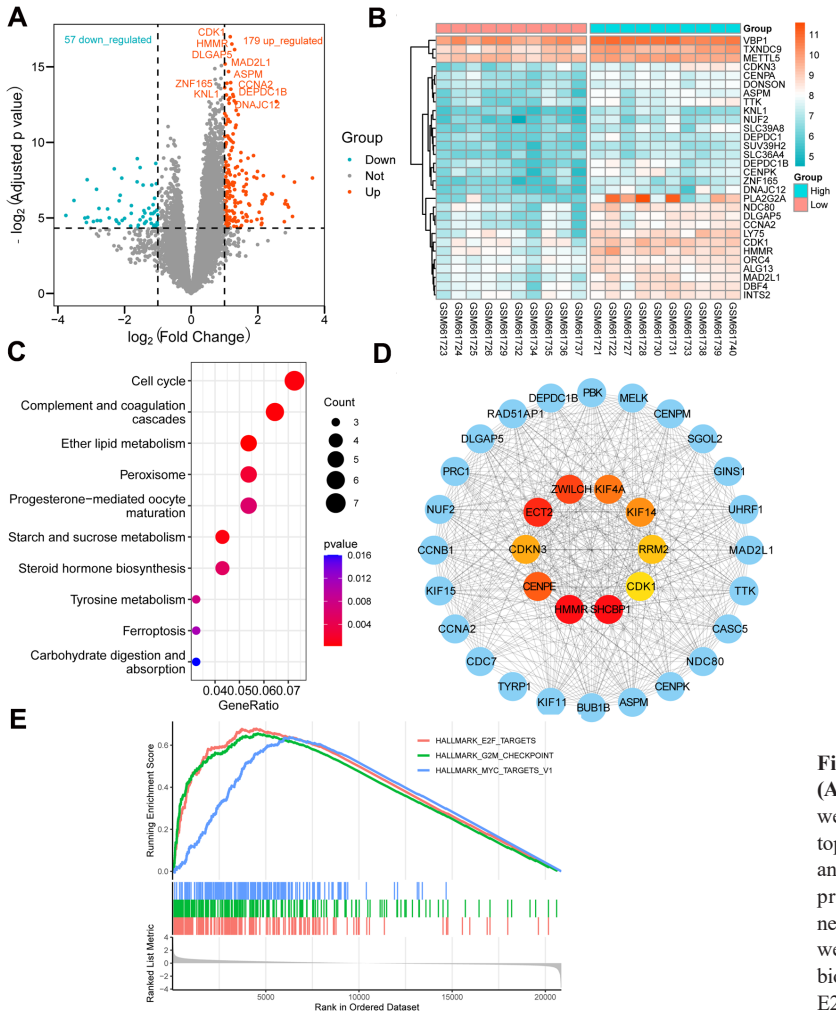

Figure 1. The results of differential analysis. **(A)** Volcano plot showed all the DEGs and top 10 were marked, while **(B)** the heatmap showed the top 30 DEGs. **(C)** Through functional enrichment analysis, it was found that cycle related biological processes were significantly enriched. **(D)** PPI network analysis was performed and ten hub genes were identified by cytoHubba. **(E)** Tumor related biological processes were significantly enriched in E2F targets and MYC targets.

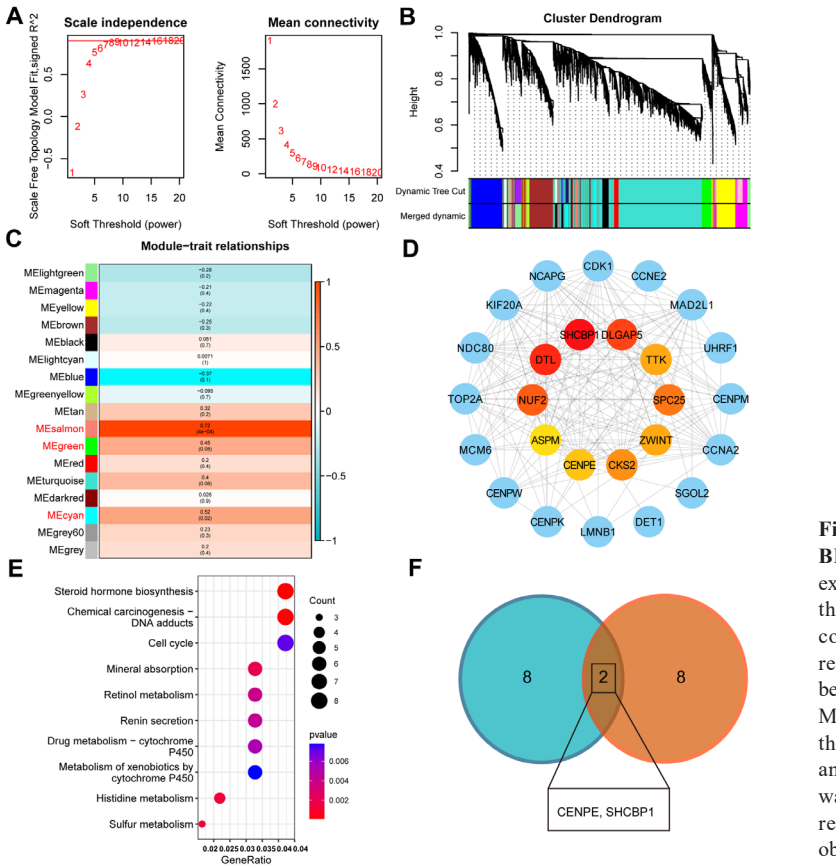

Figure 2. Cuproptosis-related gene models of BE. **(A)** The gene model was explored by co-expression analysis, and 7 was selected as the soft threshold. **(B)** Based on Spearman correlation coefficient, the heatmap of gene module-trait relationship was drawn to show the correlation between them. **(C)** Three gene models (MEsalmon, MEgreen, MEcyan) were positively corrected with the cuproptosis-related score. **(D)** PPI network analysis and **(E)** functional enrichment analysis was performed by combining all genes. **(F)** The results of DEGs and WGCNA were crossed to obtain two hub genes.

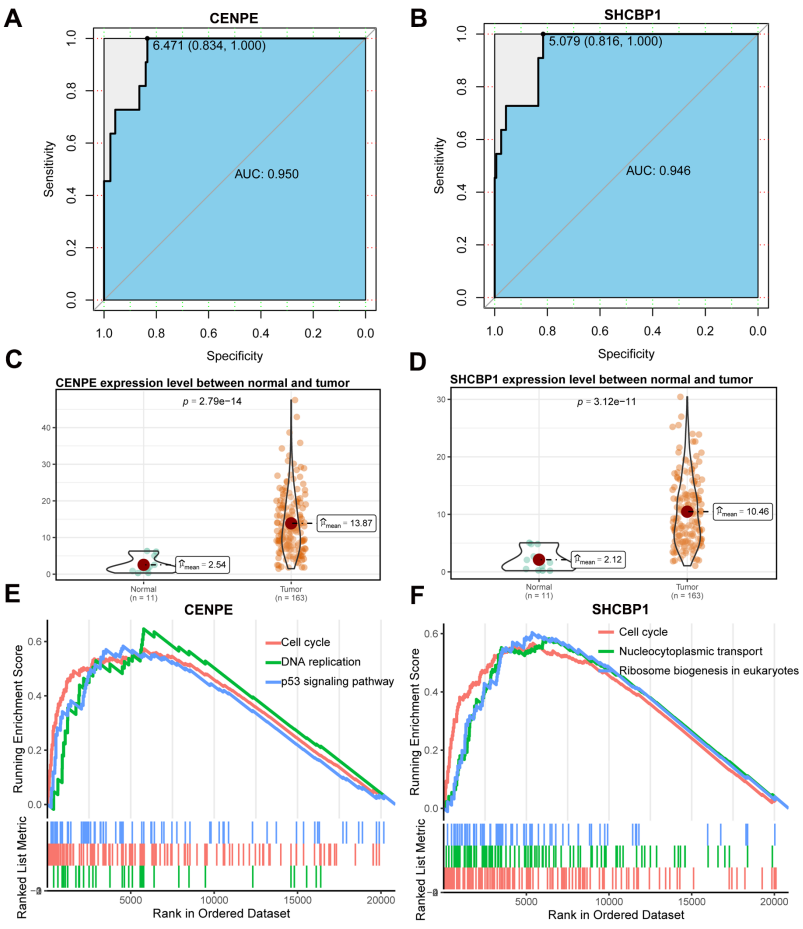

Figure 3. ROC curve and GSEA analysis based on hub gene. (A) The ROC curve AUC of CENPE could reach 0.950. **(B)** The ROC curve AUC of SHCBP1 can reach 0.946. **(C)** Both the CENPE and **(D)** SHCBP1 were expressed higher in tumor. **(E)** GSEA of CENPE and **(F)** SHCBP1 showed that cell proliferation related pathways were significantly enriched, such as cell cycle, DNA replication and p53 signaling pathway.

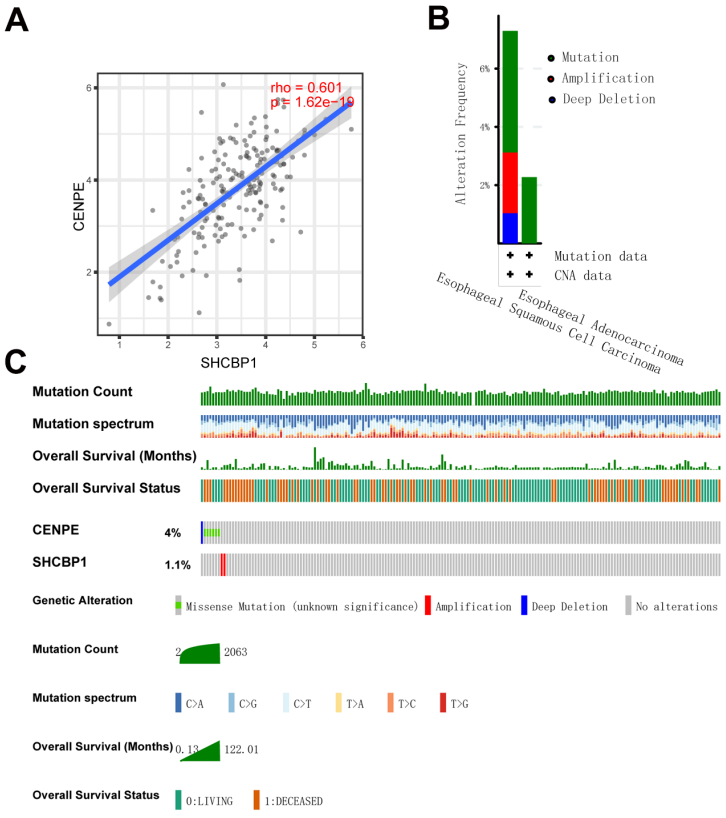

Figure 4. Mutations of CENPE and SHCBP1 in EAC. (A) CENPE was positively correlated with SHCBP1. **(B)** Genetic variants of two hub genes were present in 7% of ESC patients and 2% of EAC patients. **(C)** CENPE mutations were the most common (4%), and most were missense mutations.

we investigated the mutational landscape of two hub genes. By analyzing the cBioPortal data, seven percent of esophageal squamous cell carcinoma (ESC) patients and two percent of EAC patients had genetic alternations (Figure 4B). More specifically, mutations were most frequently identified for CENPE (4%), most of which were missense mutation (Figure 4C).

3.4. Validation of mRNA and protein levels in clinical esophageal adenocarcinoma tissues

The correlation between hub gene (*CENPE* or *SHCBP1*) expression level and clinicopathological parameters of patients was analyzed, and the results showed that CENPE was correlated with tumor stage (*P = 0.045, Table 1). Then, mRNA comparison was conducted between EAC tissues and normal tissues, and the results showed that the expressions of CENPE and SHCBP1 were significantly increased in the EAC group (*P-CENPE*<0.01, *P-SHCBP1*<0.001; Figures 5A-B). IHC results showed that the expressions of CENPE and

Table 1. Correlation between hub gene (*CENPE* or *SHCBP1*) and clinicopathological parameters in patients with EAC.

Variables	*n*	Expression of CENPE		*P* value (CENPE)	Expression of SHCBP1		*P* value (SHCBP1)
		Low	High		Low	High	
Tumors	164	73	91		69	95	
Age (years)				0.494			0.757
≤ 65	76	36	40		31	45	
> 65	88	37	51		38	50	
Sex				0.627			0.809
Male	95	35	60		45	50	
Femal	69	28	41		34	35	
Tumor stage				0.045			0.756
pT1-pT2	69	37	32		30	39	
pT3-pT4	95	36	59		39	56	
Grading				0.473			0.345
G1-G2	78	37	41		40	48	
G3-G4	86	36	50		29	47	
pN category				0.763			0.680
N0-N1	92	40	52		40	52	
N2-N3	72	33	39		29	43	
M status				0.318			0.568
M0	88	36	52		43	55	
M1	76	37	39		26	40	

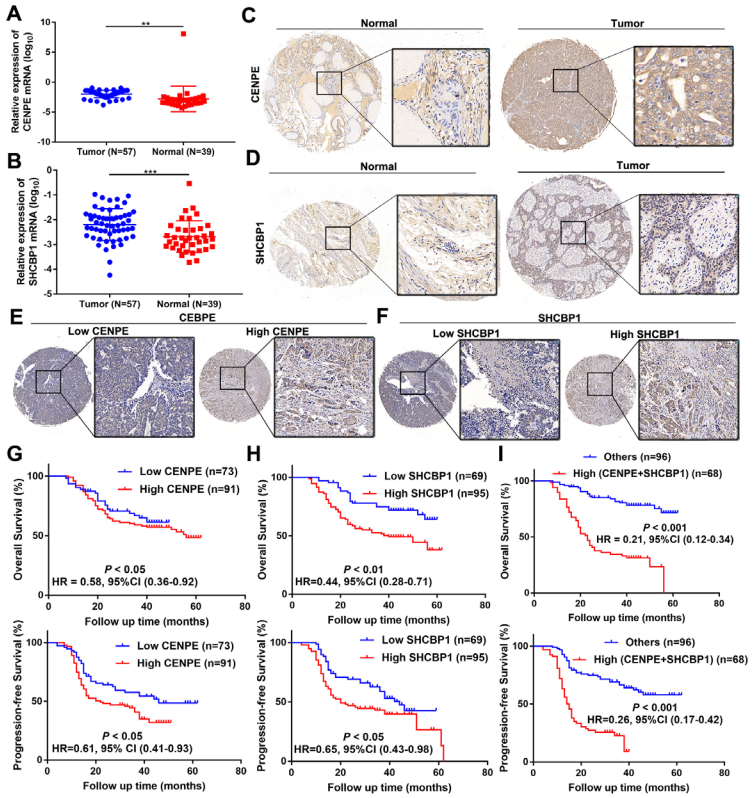

Figure 5. CENPE and SHCBP1 are overexpressed in EAC and are clinically associated with patient prognosis. (A-B) The expressions of CENPE and SHCBP1 mRNA were significantly increased in EAC tissues compared with normal tissues. **(C-D)** Immunohistochemical staining of CENPE and SHCBP1 in normal esophageal tissue and EAC. **(E-F)** Representative pictures of CENPE and SHCBP1 high and low IHC groups. **(G)** CENPE was divided into two groups according to the level of CENPE and it was found that the high expression group had a poor prognosis (*P-OS* < 0.05, HR = 0.58, 95% CI (0.36 - 0.92); *P-PFS* < 0.05, HR = 0.61, 95% CI (0.41 - 0.93). **(H)** SHCBP1 was divided into two groups according to the level of SHCBP1 and it was found that the high expression group had a poor prognosis (*P-OS* < 0.01, HR = 0.44, 95% CI (0.28 - 0.71); *P-PFS* < 0.05, HR = 0.65, 95% CI (0.43 - 0.98). **(I)** The results showed that the high CENPE and SHCBP1 protein expression group had lower OS and PFS (***P-OS* < 0.001, HR = 0.21, 95% CI (0.12 - 0.34); ***P-PFS* < 0.001, HR = 0.26, 95% CI (0.17 - 0.42)).

SHCBP1 were significantly increased in EAC (Figures 5C-D).

3.5. The expression of hub gene was negatively correlated with the prognosis of patients with EAC

EAC TMA were stained with CENPE or SHCBP1, respectively, and scored by IRS. After scoring, they were divided into high and low groups. The representative IHC pictures of CENPE and SHCBP1 are shown in Figures 5E-F. The prognostic results showed that the high expression group of CENPE had poor OS (P<0.05, HR = 0.58, 95% CI (0.36-0.92)) and PFS (P<0.05, HR = 0.61, 95% CI (0.41-0.93)), the high expression group of SHCBP1 had poor OS (P<0.01, HR = 0.44, 95% CI (0.28-0.71)) and PFS (P<0.05, HR = 0.65, 95% CI (0.43-0.98)), and the OS (P<0.001, HR = 0.21, 95% CI (0.12-0.34))and PFS (P<0.001, HR = 0.26, 95% CI (0.17-0.42)) of patients with high expression of CENPE and SHCBP1 was worse than that of other patients (Figure 5G-I).

3.6. CENPE and SHCBP1 can induce cuproptosis in EAC

Knocking down CENPE or SHCBP1 significantly inhibited the growth of Eca109 and KYSE450 cells (Figure 6A). Knocking down CENPE, SHCBP1, $CuCl_2$ treatment or elesclomol-$CuCl_2$ promoted Eca109 cells death alone, and combined with CuCl2 or elesclomol-$CuCl_2$ aggravated the cell death in Eca109 cells (Figure 6B). The copper accumulation increased after Knocking down CENPE or SHCBP1 in Eca109 cells, also suggesting that copper is involved these two genes induced cell death (Figure 6C). Next, the mRNA and protein expression of the copper import gene SLC31A1 was increased after knocking down CENPE or SHCBP1 with or without $Cucl_2$ (Figure 6D).

3.7. Association between cuproptosis-related score and immune infiltration

Firstly, seven different immune infiltration algorithms were utilized to calculate the immune infiltration landscape (Figure S3, *http://www.biosciencetrends.com/action/getSupplementalData.php?ID=171*). As shown in Figure 7A, there were more immune cell infiltrates in the low cuproptosis-related score group, especially the T cells. Then relationship between the level of immune infiltration and two hub genes (CENPE, SHCBP1) were estimated. It was found that both two hub genes positively correlated with Neutrophil and Myeloid dendritic cell (Figure 7B-C).

3.8. Single cell sequencing analysis

In order to confirm the functions of CENPE and SHCBP1, single cell-seq data were analyzed. After quality control (Figures S4A-E, *http://www.biosciencetrends.com/action/getSupplementalData.php?ID=171*), all 34,706 cells were retained for t-SNE analysis. Based on the signature gene expression, 19 cell clusters were annotated (Figure 8A). According to the well-known marker genes (Figure S4F, *http://www.biosciencetrends.com/action/getSupplementalData.php?ID=171*), we designated all clusters as pre-myeloid cells, epithelial, fibroblasts, NK and T cells, endothelial, neutrophils and B cells (Figure 8B). Interestingly, we found CENPE and SHCBP1 were co-expressed in a special NK and T sub cell type (Figures 8C-D). Next,

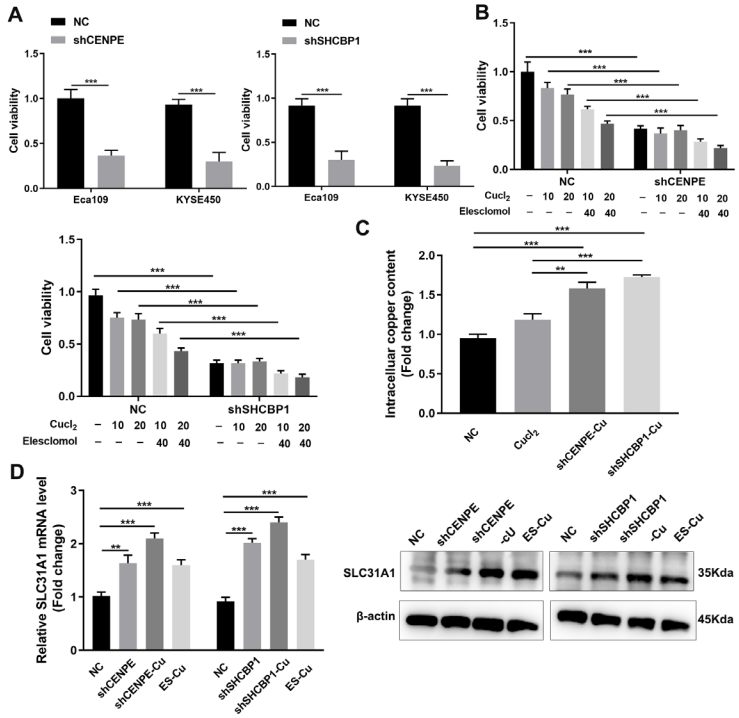

Figure 6. CENPE and SHCBP1 can induce cuproptosis in EAC. (A) Knocking down CENPE or SHCBP1 significantly inhibited the growth of Eca109 and KYSE450 cells. **(B)** Viability of Eca109 cells after knocking down CENPE or SHCBP1, or indicated elesclomol-Cu treatment. **(C)** Intracellular copper content in EAC cells after knocking down CENPE or SHCBP1, or $Cucl_2$ (10μM) treatment. **(D)** mRNA levels and protein levels of copper ion transporter in Eca109 cells after knocking down CENPE or SHCBP1, or ES-Cu treatment.

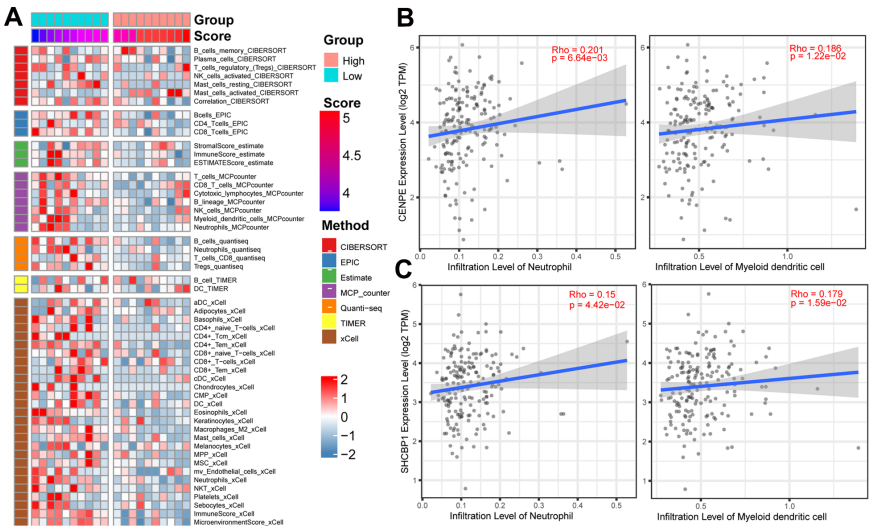

Figure 7. Association between cuproptosis-related score and immune infiltration. (A) There were more immune cell infiltrates in the low cuproptosis-related score group, especially the T cells. **(B-C)** By assessing the relationship between immune infiltration levels and two central genes (CENPE, SHCBP1), we found that both neutrophils and myeloid dendritic cells were able to positively correct both hub genes.

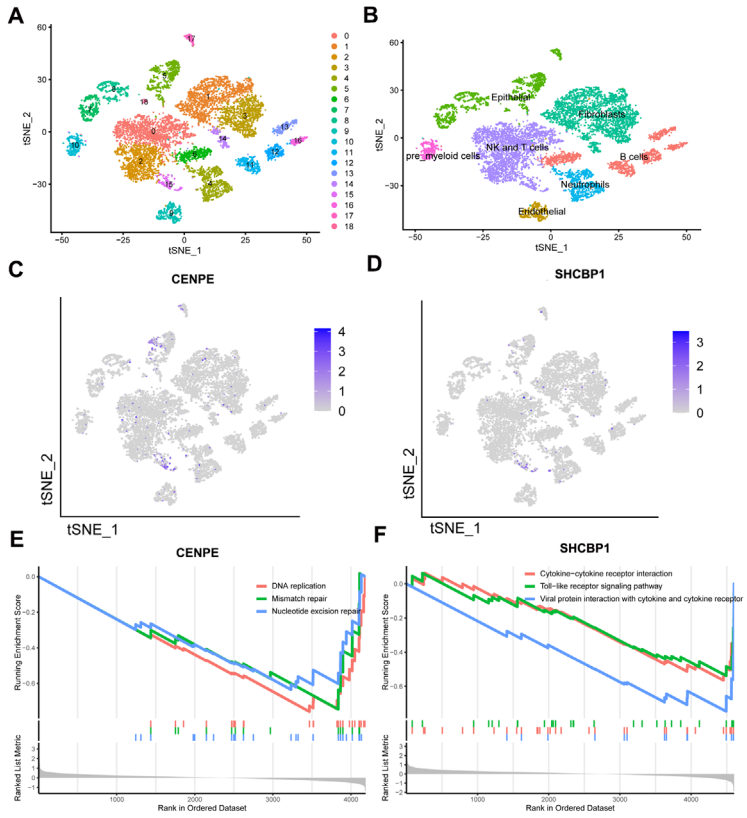

Figure 8. The function of CENPE and SHCBP1. (A) Single cell sequence data sequencing revealed that 34,706 cells were used for t-SNE analysis and 19 cell clusters were annotated based on characteristic gene expression. **(B)** According to the well-known marker genes, we designated all clusters as pre-myeloid cells, epithelial, fibroblasts, NK and T cells, endothelial, neutrophils and B cells. **(C-D)** CENPE and SHCBP1 can be co-expressed in a specific NK and T subcell type**. (E)** CENPE is associated with biological processes related to DNA repair and **(F)** SHCBP1 is associated with biological processes related to inflammation or immunity.

GSEA analysis was performed to uncover the function of two hub genes in this sub cell type. It was showed that CENPE corrected with DNA repair-related biological processes and SHCBP1 corrected with inflammation or immune related biological processes (Figures 8E-F). We considered that CENPE and SHCBP1 might be related to the immune function of NK cells and T cells.

4. Discussion

BE is one of the most common premalignant lesions in which normal squamous epithelium of the esophagus is replaced by metaplastic columnar epithelium. EAC develops through progression from BE to low-grade and high-grade dysplasia (LGD/HGD) and to adenocarcinoma (*40,41*). Previous studies found that the incidence of EAC in patients with BE was 11.34 times higher than that in the general population (*42*). Cuproptosis is a recently discovered form of cell death that occurs due to an excess of copper ions in cells, resulting in the generation of reactive oxygen species and oxidative stress. This process can lead to various types of cellular damage and ultimately cell death (*19*). Targeting copper cytotoxicity and cuproptosis are considered potential options for treating oncological diseases.

In this study, we used ssGSEA to calculate

cuproptosis-related scores of BE patients. Based on the score, two hub genes (CENPE and SHCBP1) were identified by differential gene analysis and WGCNA. We further targeted at these two hub genes to predict EAC by ROC curve, and the AUC could reach 0.950 and 0.946 respectively. Bioinformatics analysis showed that the expression of these two genes was significantly increased in EAC. In addition, mutations of these two genes in esophageal cancer were analyzed. Genetic variants were found in 7% of patients with ESC and 2% of patients with EAC.

We further verified the expression of these two genes in clinical tissues of EAC, and found that the mRNA and protein levels of CENPE and SHCBP1 were significantly increased. The two hub genes were grouped by protein expression level, and the results showed that patients with high CENPE expression, high SHCBP1 expression or both high expression groups had poor prognosis. Previous studies have reported that CENPE was increased in EAC, but only at the mRNA level, with a very limited sample size. At the same time, CENPE was negatively correlated with prognostic OS, while other prognostic PFS were not involved, and the sample follow-up data was poor (*11*). The reports on SHCBP1 are only database-based results, and mRNA and protein levels have not been verified in clinical samples (*14*). In this study, we made full use of our tumor center's powerful clinical sample bank and patient follow-up data to analyze mRNA and protein levels and prognosis. These findings suggest that cuproptosis-related CENPE and SHCBP1 genes may promote the development of BE into EAC, and may be a poor prognostic factor for patients. In addition, we further verified in esophageal cancer cells that CENPE and SHCBP1 can cause cuproptosis and are hub genes associated with cuproptosis. At present, the study of CENPE and SHCBP1 genes in BE and the transformation of BE to EAC has not been reported.

DNA damage, genetic changes and chronic inflammation have also been reported to be important factors in the development of epigenetic changes in BE (*43*). The process of cuproptosis is also accompanied by an inflammatory response (*7*). In order to confirm the function of CENPE and SHCBP1 in EAC, we analyzed the relationship between CENPE and SHCBP1 genes and inflammatory immunity. The results showed that the infiltration of immune cells, especially T cells, was more in the group with low copper death score. Previous studies have reported that SHCBP1 is significantly associated with CD8+ T cell infiltration, cytokines, cytokine receptors, MHC genes and multiple immune antigens in pancarcinoma (*14*). In addition, CENPE was strongly associated with SHCBP1, and they were strongly associated with neutrophil or myeloid dendritic cell infiltration.

Epigenetically inactivated genes in BE were found to be involved in important molecular pathways of tumorigenesis, including cell cycle regulation, apoptosis, DNA repair, antioxidative defense, or cell adhesion (*44-49*). Single-cell RNA sequencing has become a powerful tool to characterize different functional states at single-cell resolution and is widely used in cancer research (*50,51*). By single cell sequencing, CENPE and SHCBP1 were co-expressed in NK and T cells. GSEA analysis showed that CENPE was negatively correlated with DNA repair and SHCBP1 was negatively correlated with biological

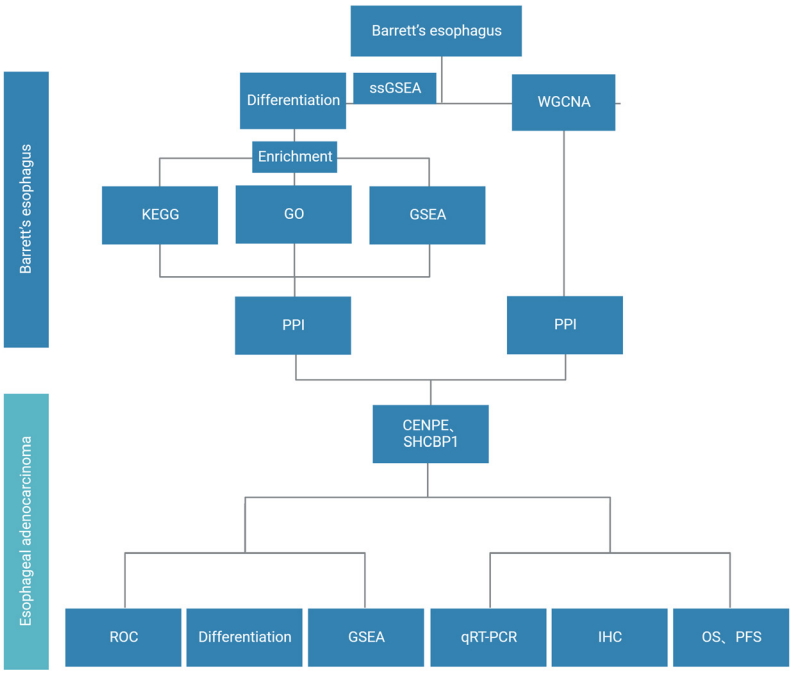

Figure 9. Flow diagram of full text.

processes related to inflammation and immunity. Therefore, CENPE and SHCBP1 may associated with the immune function of NK cells and T cells.

The main line of this paper is original, which starts from the clinical BE, which excavates the gene module related to cuproptosis. Through difference analysis, survival analysis, and ROC analysis, BE and EAC are connected through the copper death gene, which indicates which BE may develop into EAC (Figure 9). Therefore, early screening and biopsy analysis of BE can avoid the occurrence of EAC, which is of great clinical transformation value.

In conclusion, the hub gene (CENPE and SHCBP1) associated with cuproptosis may be a factor promoting the development of BE into EAC which associated with the regulation of NK cells and T cells.

Acknowledgements

We are grateful to all those who helped with this project.

Funding: This work was supported, in part, by grants from the National Natural Science Foundation of China (No. 81972431, 82272898); Shanghai Anticancer Association EYAS PROJECT (No. SACA-CY19A07); and the Female Tumour Project of Shanghai Key Clinical Specialty (No. SHSLCZDZK06301).

Conflict of Interest: The authors have no conflicts of interest to disclose.

References

1. Martinez P, Mallo D, Paulson TG, Li XH, Sanchez CA, Reid BJ, Graham TA, Kuhner MK, Maley CC. Evolution of Barrett's esophagus through space and time at single-crypt and whole-biopsy levels. Nat Commun. 2018; 9:794.
2. Guillem PG. How to make a Barrett esophagus: pathophysiology of columnar metaplasia of the esophagus. Dig Dis Sci. 2005; 50:415-424.
3. Wild CP, Hardie LJ. Reflux, Barrett's oesophagus and adenocarcinoma: burning questions. Nat Rev Cancer. 2003; 3:676-684.
4. Brown CS, Ujiki MB. Risk factors affecting the Barrett's metaplasia-dysplasia-neoplasia sequence. World J Gastrointest Endosc. 2015; 7:438-445.
5. Keswani T, Mitra S, Bhattacharyya A. Copper-induced immunotoxicity involves cell cycle arrest and cell death in the liver. Environ Toxicol. 2015; 30:411-421.
6. Liu J, Liu Y, Wang Y, Kang R, Tang D. HMGB1 is a mediator of cuproptosis-related sterile inflammation. Front Cell Dev Biol. 2022; 10:996307.
7. Zhao J, Guo S, Schrodi SJ, He D. Cuproptosis and cuproptosis-related genes in rheumatoid arthritis: Implication, prospects, and perspectives. Front Immunol. 2022; 13:930278.
8. Jiang R, Sun Y, Li Y, Tang X, Hui B, Ma S, Zhang J, Sun C, Tan J, Zhou B, Lei J, Jiang T. Cuproptosis-related gene PDHX and heat stress-related HSPD1 as potential key drivers associated with cell stemness, aberrant metabolism and immunosuppression in esophageal carcinoma. Int Immunopharmacol. 2023; 117:109942.
9. Bao JH, Lu WC, Duan H, Ye Y, Li J, Liao W, Li Y, Sun Y. Identification of a novel cuproptosis-related gene signature and integrative analyses in patients with lower-grade gliomas. Front Immunol. 2022; 13:933973.
10. Huang J, Zhang J, Wang F, Zhang B, Tang X. Comprehensive analysis of cuproptosis-related genes in immune infiltration and diagnosis in ulcerative colitis. Front Immunol. 2022; 13:1008146.
11. Zhu X, Luo X, Feng G, Huang H, He Y, Ma W, Zhang C, Zeng M, Liu H. CENPE expression is associated with its DNA methylation status in esophageal adenocarcinoma and independently predicts unfavorable overall survival. PLoS One. 2019; 14:e0207341.
12. Shan L, Zhao M, Lu Y, Ning H, Yang S, Song Y, Chai W, Shi X. CENPE promotes lung adenocarcinoma proliferation and is directly regulated by FOXM1. Int J Oncol. 2019; 55:257-266.
13. Hao X, Qu T. Expression of CENPE and its Prognostic Role in Non-small Cell Lung Cancer. Open Med (Wars). 2019; 14:497-502.
14. Wang N, Zhu L, Wang L, Shen Z, Huang X. Identification of SHCBP1 as a potential biomarker involving diagnosis, prognosis, and tumor immune microenvironment across multiple cancers. Comput Struct Biotechnol J. 2022; 20:3106-3119.
15. Huang Y, You M, Wu Q, Zhu W, Guo F, Lin W. SHCBP1 Is a Prognostic Biomarker Related to the Tumour Immune Microenvironment in Pan-Cancer. Ann Clin Lab Sci. 2022; 52: 904-917.
16. Jiang F, Shi Y, Wang Y, Ge C, Zhu J, Fang H, Zhang Y, Zhang Y, Jian H, Lei T, Lan S, Cao L, Yu H, Fang D. Characterization of SHCBP1 to prognosis and immunological landscape in pan-cancer: novel insights to biomarker and therapeutic targets. Aging (Albany NY). 2023; 15:2066-2081.
17. Cao J, Yu C. Identification of Immune Infiltration and Prognostic Biomarkers in Small Cell Lung Cancer Based on Bioinformatic Methods from 3 Studies. Comb Chem High Throughput Screen. 2023; 26:507-516.
18. Dong Z, Wang J, Zhang H, Zhan T, Chen Y, Xu S. Identification of potential key genes in esophageal adenocarcinoma using bioinformatics. Exp Ther Med. 2019; 18:3291-3298.
19. Tsvetkov P, Coy S, Petrova B, *et al*. Copper induces cell death by targeting lipoylated TCA cycle proteins. Science. 2022; 375:1254-1261.
20. Hanzelmann S, Castelo R, Guinney J. GSVA: gene set variation analysis for microarray and RNA-seq data. BMC Bioinformatics. 2013; 14:7.
21. Wang W, Xu SW, Zhu XY, Guo Q, Zhu M, Mao X, Chen Y, Li S, Luo W. Identification and validation of a novel RNA-binding protein-related gene-based prognostic model for multiple myeloma. Front Genet. 2021; 12:665173.
22. Langfelder P, Horvath S. WGCNA: an R package for weighted correlation network analysis. BMC Bioinformatics. 2008; 9:559.
23. Ashburner M, Ball CA, Blake JA, *et al*. Gene ontology: tool for the unification of biology. The gene ontology consortium. Nat Genet. 2000; 25:25-29.
24. Kanehisa M, Goto S. KEGG: kyoto encyclopedia of genes and genomes. Nucleic Acids Res. 2000; 28:27-30.
25. Subramanian A, Tamayo P, Mootha VK, Mukherjee S, Ebert B, Gillette MA, Paulovich A, Pomeroy SL, Glolub

TR, Lander ES, Mesirov JP. Gene set enrichment analysis: a knowledge-based approach for interpreting genome-wide expression profiles. Proc Natl Acad Sci U S A. 2005; 102:15545-15550.
26. Gurbuz BC, Topal CS, Sobay R, Alkurt G, Zemheri IE. Molecular and immunohistochemical evaluation of BAP-1 antibody in bladder cancer and comparison with luminal-basal subtyping. Pathol Res Pract. 2021; 217:153308.
27. Wu J, Wu Y, Guo Q, Chen S, Wang S, Wu X, Zhu J, Ju X. SPOP promotes cervical cancer progression by inducing the movement of PD-1 away from PD-L1 in spatial localization. J Transl Med. 2022; 20:384.
28. Wu J, Wang R, Ye Z, Sun X, Chen Z, Xia F, Sun Q, Liu L. Protective effects of methane-rich saline on diabetic retinopathy *via* anti-inflammation in a streptozotocin-induced diabetic rat model. Biochem Biophys Res Commun. 2015; 466:155-161.
29. Kolodziej-Rzepa M, Biesaga B, Slonina D, Mucha-Malecka A. Nanog expression in patients with squamous cell carcinoma of oropharynx in relation to immunohistochemical score. Pol J Pathol. 2022; 73:60-71.
30. Hofmann M, Stoss O, Shi D, Ruttner R, Vijver M, Kim W, Ochiai A, Ruschoff J, Henkel T. Assessment of a HER2 scoring system for gastric cancer: results from a validation study. Histopathology. 2008; 52:797-805.
31. Krishnamurthy N, Goodman AM, Barkauskas DA, Kurzrock R. STK11 alterations in the pan-cancer setting: prognostic and therapeutic implications. Eur J Cancer. 2021; 148:215-229.
32. Bellone S, Roque DM, Siegel ER, *et al*. A phase 2 evaluation of pembrolizumab for recurrent Lynch-like versus sporadic endometrial cancers with microsatellite instability. Cancer. 2022; 128:1206-1218.
33. Petrelli F, Cortellini A, Indini A, *et al*. Association of obesity with survival outcomes in patients with cancer: A systematic review and meta-analysis. JAMA Netw Open. 2021; 4:e213520.
34. Zeng D, Ye Z, Shen R, Yu G, Wu J, Xiong Y, Zhou R, Qiu W, Huang N, Sun L, Li X, Bin J, Liao Y, Shi M, Liao W. IOBR: Multi-omics immuno-oncology biological research to decode tumor microenvironment and signatures. Front Immunol. 2021; 12:687975.
35. Ali BM, Azmeh AM, Alhalabi NM. Suprachoroidal triamcinolone acetonide for the treatment of macular edema associated with retinal vein occlusion: A pilot study. BMC Ophthalmol. 2023; 23:60.
36. Hao Y, Hao S, Andersen-Nissen E, *et al*. Integrated analysis of multimodal single-cell data. Cell. 2021; 184:3573-3587 e29.
37. Lee S, Chen D, Park M, Kim S, Choi Y, Moon S, Shin D, Lee J, Kim E. Single-cell RNA sequencing analysis of human dental pulp stem cell and human periodontal ligament stem cell. J Endod 2022; 48:240-248.
38. Zhang Z, Zhu H, Zhao C, Liu D, Luo J, Ying Y, Zhong Y. DDIT4 promotes malignancy of head and neck squamous cell carcinoma. Mol Carcinog. 2023; 62:332-347.
39. Zheng M, Hu Y, Liu O, Li S, Wang Y, Li X, Liu J, Yng Q, Li X, Lin B. Oxidative stress response biomarkers of ovarian cancer based on single-cell and bulk RNA sequencing. Oxid Med Cell Longev. 2023; 2023:1261039.
40. Barrett NR. Chronic peptic ulcer of the oesophagus and 'oesophagitis'. Br J Surg. 1950; 38:175-182.
41. Shaheen NJ, Falk GW, Iyer PG, Gerson LB, American College of G. ACG clinical guideline: Diagnosis and management of Barrett's Esophagus. Am J Gastroenterol. 2016; 111:30-50; quiz 1.
42. Bhat S, Coleman HG, Yousef F, Johnston BT, McManus DT, Gavin AT, Murray LJ. Risk of malignant progression in Barrett's esophagus patients: results from a large population-based study. J Natl Cancer Inst. 2011; 103:1049-1057.
43. Kundu JK, Surh YJ. Inflammation: gearing the journey to cancer. Mutat Res. 2008; 659:15-30.
44. Kuester D, El-Rifai W, Peng D, Ruemmele P, Kroeckel L, Peters B, Moskaluk CA, Stolte M, Monkemuller K, Meyer F, Schulz HU, Hartmann A, Roessner A, Schneider R. Silencing of MGMT expression by promoter hypermethylation in the metaplasia-dysplasia-carcinoma sequence of Barrett's esophagus. Cancer Lett. 2009; 275:117-126.
45. Kuester D, Dar AA, Moskaluk CC, Krueger SK, Meyer F, Hartig R, Stolte M, Malfertheiner P, Lippert H, Roessner A, EI-Rifai W, Schneider-stock R. Early involvement of death-associated protein kinase promoter hypermethylation in the carcinogenesis of Barrett's esophageal adenocarcinoma and its association with clinical progression. Neoplasia. 2007; 9:236-245.
46. Kuroki T, Trapasso F, Yendamuri S, Matsuyama A, Alder H, Mori M, Croce CM. Promoter hypermethylation of RASSF1A in esophageal squamous cell carcinoma. Clin Cancer Res. 2003; 9:1441-1445.
47. Ohki R, Nemoto J, Murasawa H, Oda E, Inazawa J, Tanaka N, Taniguchi T. Reprimo, a new candidate mediator of the p53-mediated cell cycle arrest at the G2 phase. J Biol Chem. 2000; 275:22627-22630.
48. Wang JS, Guo M, Montgomery EA, Thompson RE, Cosby H, Hicks L, Wang S, Herman JG, Canto MI. DNA promoter hypermethylation of p16 and APC predicts neoplastic progression in Barrett's esophagus. Am J Gastroenterol. 2009; 104:2153-2160.
49. Klump B, Hsieh CJ, Holzmann K, Gregor M, Porschen R. Hypermethylation of the CDKN2/p16 promoter during neoplastic progression in Barrett's esophagus. Gastroenterology. 1998; 115:1381-1386.
50. Ye F, Huang W, Guo G. Studying hematopoiesis using single-cell technologies. J Hematol Oncol. 2017; 10:27.
51. Ren X, Kang B, Zhang Z. Understanding tumor ecosystems by single-cell sequencing: Promises and limitations. Genome Biol. 2018; 19:211.

Received July 12, 2023; Revised October 10, 2023; Accepted October 15, 2023.

[§]These authors contributed equally to this work.
**Address correspondence to:*
Jiangchun Wu, Department of Gynecologic Oncology, Fudan University Shanghai Cancer Center, Fudan University, Shanghai 200032, China.
E-mail: drwujiangchun2019@hotmail.com

Released online in J-STAGE as advance publication October 21, 2023.